

SUPPLEMENTARY INFORMATION

High Trap Stiffness Microcylinders for Nanophotonic Trapping

Ryan P. Badman¹, Fan Ye^{1,2}, Wagma Caravan^{1,3}, and Michelle D. Wang^{1,2,}*

¹Department of Physics – LASSP, Cornell University, Ithaca, New York 14853.

²Howard Hughes Medical Institute, Cornell University, Ithaca, New York 14853.

³Department of Chemistry, Adelphi University, Garden City, NY 11530

**corresponding author: mwang@physics.cornell.edu*

Summary

Figure S1: Cartoon schematic of the material layers of the microparticles under study.

Figure S2: Simulations of the maximum force along all three directions for each watt of laser power at the nSWAT trapping region.

Figure S3: Calculated maximum force along z for microspheres of five different microparticle materials.

Figure S4: Simulations of the dependence of the maximum trapping force along z as a function of microcylinder dimensions for (a) lift-off and (b) cleaved microcylinders.

Figure S5: Trap stiffness enhancement contributions from geometry and refractive index.

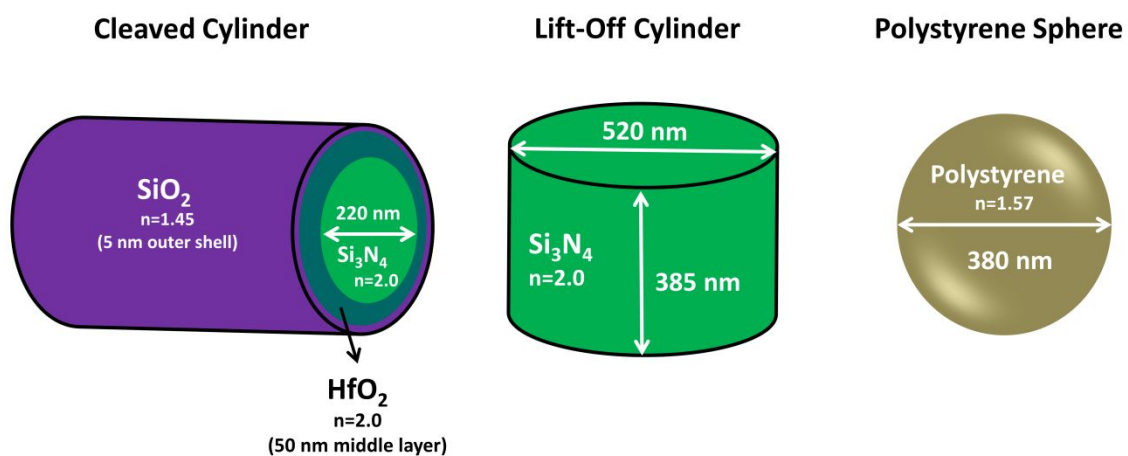


Figure S1: Cartoon schematic of the composition of each microparticle under study. Shown are the mean dimensions.

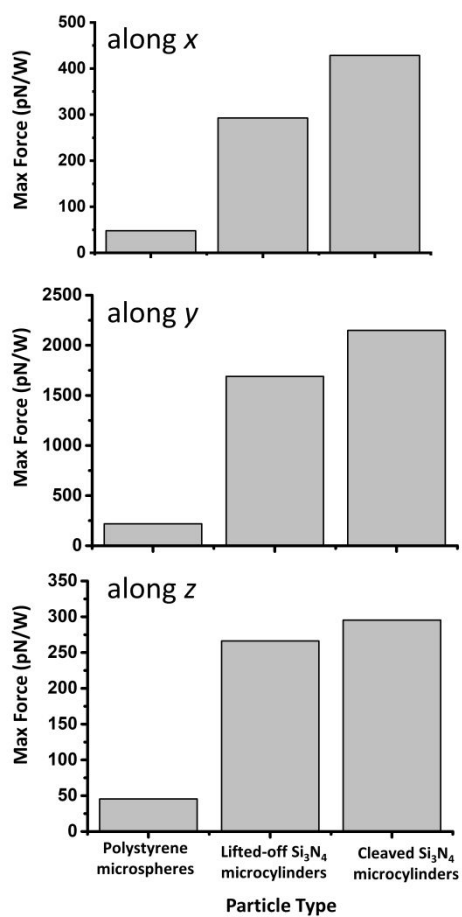


Figure S2: Simulations of the maximum force along all three directions for each watt of laser power at the nSWAT trapping region. Note the trap stiffness enhancement of the microcylinders over microspheres in all three directions.

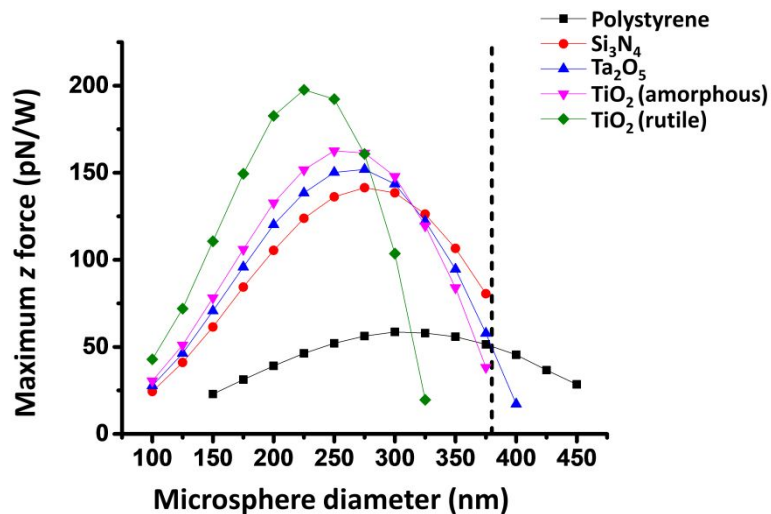


Figure S3: Calculated maximum force along z for microspheres of five different microparticle materials: polystyrene ($n = 1.57$ at 1064 nm), Si₃N₄ ($n = 2.0$), amorphous Ta₂O₅ ($n = 2.15$), amorphous TiO₂ ($n = 2.25$), and rutile TiO₂ ($n = 2.75$). These simulations show that higher refractive index microspheres provide substantially larger force enhancement with the maximum enhancement occurring at a smaller diameter. The vertical dashed line indicates the diameter of the polystyrene microspheres used in this work.

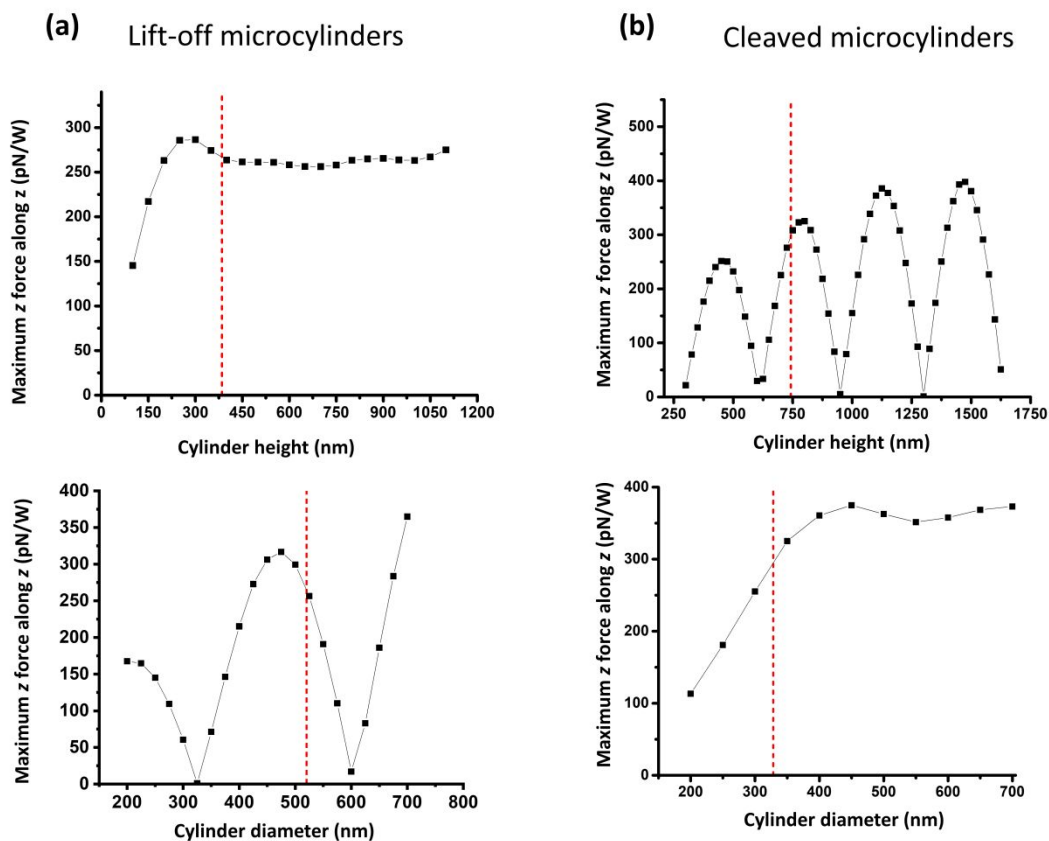


Figure S4: Simulations of the dependence of the maximum trapping force along z as a function of microcylinder dimensions for (a) lift-off and (b) cleaved microcylinders. In each simulation, only a single dimension was varied while the other dimension was held at the mean value, and the cylinder orientation was also held fixed. Each vertical dashed line indicates the mean fabricated dimension.

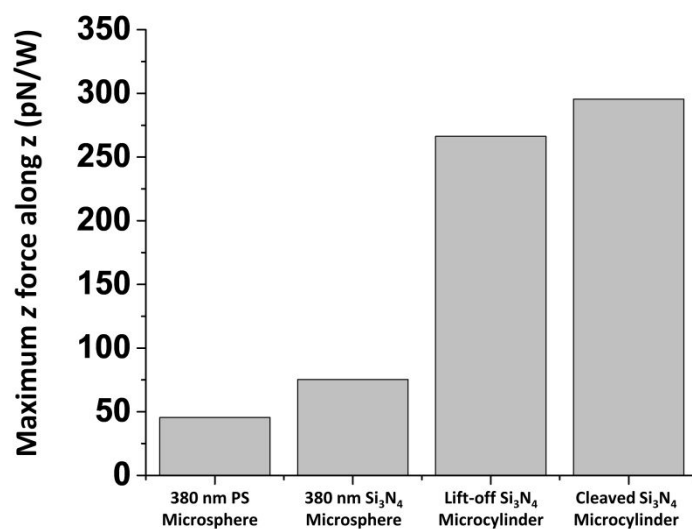


Figure S5: Trap stiffness enhancement contributions from refractive index and geometry. We computed the maximum z trapping forces for a 380 nm diameter polystyrene microsphere, a 380 nm diameter Si₃N₄ microsphere (also see Figure S3), a lift-off Si₃N₄ microcylinder (also see Figure 3), and a cleaved Si₃N₄ microcylinder (also see Figure 3). The mean measured dimensions for cleaved microcylinders and lift-off microcylinders were used in the simulations.